Low-temperature variational approximation for the Feynman quantum propagator and its application to the simulation of quantum systems

Jianshu Cao and B. J. Berne
Department of Chemistry, Columbia University, New York, New York 10027

(Received 24 October 1989; accepted 8 February 1990)

The low-temperature propagator of Mak and Andersen [J. Chem. Phys. **92**, 2953 (1990)] allows for much more rapid convergence of Feynman path integral computer simulations of quantum systems. The effectiveness of this propagator is very sensitive to the choice of an effective frequency and the choice of this made by Mak and Andersen, although good, is not optimum. In this paper a harmonic reference system is used together with a variation principle to compute this effective frequency. Simulations show that when this is used in the low temperature propagator, the results converge much more rapidly than for other choices of the frequency. Moreover, an energy estimator is derived, which allows this effective potential to be used for the determination of the energy of the quantum system. In addition, using a cumulant expansion of the centroid density in the free particle reference system, an effective potential along with a corresponding energy estimator is derived and compared to the above.

I. INTRODUCTION

Feynman path integral methods provide a powerful tool for studying the equilibrium thermodynamics of quantum system.[1] The Trotter theorem makes it possible to discretize the path integral[2,3] such that the statistical mechanics of a quantum particle becomes isomorphic to that of a classical polymer chain of P beads. This permits one to devise algorithms for the numerical simulation of quantum systems.[1-4] As P increases, the thermal properties of the polymer chain will asymptotically approach that of the quantum particle. If more accurate propagators are used, the simulation will converge more rapidly to the exact result and smaller P will suffice. This observation has inspired the quest for more accurate short-time propogators. Examples are the generalized Trotter formula which is based on a higher order operator expansion,[5] the exponential power series expansion which is a recursion integral relation directly derived from the Bloch equation,[6] the variable quadratic propagator which combines the features of the Taylor expansion and the quasiharmonic approximation,[7] and finally, the low temperature propagator designed to generate good accuracy for bound systems at low temperatures.[8] All of these improvement significantly reduce the required central processing unit (cpu) time while assuring convergence of simulation.

The original and most commonly used thermal propagator, correct to the first order in β, follows directly from the Trotter formula[2,3]

$$\rho(x,x';\beta) = \sqrt{\frac{m}{2\pi\hbar^2\beta}} \exp - S, \tag{1.1}$$

where the exponential part S is the dimensionless imaginary time action which is approximated by

$$S = \frac{m}{2\hbar^2\beta}(x-x')^2 + \beta\left[\frac{V(x)+V(x')}{2}\right]. \tag{1.2}$$

Because this is only accurate at high temperature, we shall call it the high temperature propagator (HT propagator).

Mak and Andersen[8] devised a low temperature propagator (LT propagator)

$$\rho(x,x';\beta) = \sqrt{\frac{m}{2\pi\hbar^2\beta}}\left(\frac{\alpha}{\sinh(\alpha)}\right)^{1/2} \exp - S, \tag{1.3}$$

where

$$S = \frac{m}{2\hbar^2\beta}\frac{\alpha}{\sinh(\alpha)}(x-x')^2 + \beta\frac{\tanh(\alpha/2)}{(\alpha/2)}\left[\frac{V(x)+V(x')}{2}\right], \tag{1.4}$$

$\alpha = \beta\hbar\omega$, and where the effective frequency ω is determined either from:

(a) the curvature at the minimum of the potential

$$m\omega^2 = V''(x_0), \tag{1.5}$$

or from;

(b) the normalization condition of the effective LHO at infinitely low temperature, i.e.,

$$\int_{-\infty}^{\infty} \exp\left(-\frac{2V(x)}{\hbar\omega}\right) dx = \sqrt{\frac{\pi\hbar}{m\omega}}. \tag{1.6}$$

Equation (1.3) reduces to the HT propagator [Eq. (1.1)] at high temperature and moreover when it is applied to the linear harmonic potential $V(x) = m\omega^2/2$, it gives the exact propagator at all temperatures for $\omega = \omega_0$. Of the two prescriptions for determining the effective frequency, method (b) is preferable, especially for the case where the curvature of the potential at its minimum (a) is zero. However, both (a) and (b) serve merely as convenient *ad hoc* choices of the effective frequency. As we shall show, there are better choices. The low temperature propagator can be generalized to many-degree-of-freedom systems and to the computation of thermal time correlation functions.

Feynman[2] introduced an effective classical potential which includes quantum corrections and used it to calculate the quantum statistical properties in the canonical ensemble. He introduced the centroid density and evaluated it by averaging all isomorphic polymer chains (quantum paths) with barycenter fixed at a given position. Feynman performs his

 0021-9606/90/127531-09$03.00

averages using a free particle reference system. Following Feynman, using cumulant methods, we obtain a general form for the effective potential which in principle includes all quantum corrections. Keeping only the first few leading terms, we are able to generate a very accurate approximation to the effective potential.

Feynman[9] has also exploited a local harmonic reference system to determine the statistical properties of systems with arbitrary potential functions. He determines the effective frequency to be used in the reference system by using a variation principle based on the Gibbs–Bogiliubov inequality and with this approximates the partition function of a quantum particle. Recently, Voth *et al.*[10] used the same basic idea to study barrier crossing problems. This approach allows us to derive a simple and explicit equation for the effective frequency to be used in place of methods (a) and (b) in Mak and Andersen's LT propagator. This yields a very rapidly convergent approximation to the low temperature propagator defined in Eq. (1.3). We introduce a perturbation solution for the effective frequency which clarifies the relation between the effective potential based on the free particle reference systems (discussed in the previous paragraph) and the effective quadratic potential based on the harmonic reference system. This also allows us to derive explicit expressions for the energy estimators corresponding in these two reference systems, and thereby use these approaches in Monte Carlo simulations to determine the energy. The second method is shown to be very accurate when applied to bound systems in the low temperature limit.

In the low temperature propagator [Eq. (1.3)], the spread of convergence depends strongly on the effective frequency ω. The form of ω determined from the effective quadratic potential approximation is a very attractive choice as it springs from a physical derivation rather than the imposition of an arbitrary normalization condition. We present several numerical simulations to show that this choice of the frequency is superior to the others in that it leads to much more rapid convergence than the original choices made by Mak *et al.*

II. THEORY

A. The unnormalized centroid density

The canonical partition function can be expressed as[2]

$$Z=\int \rho(x_0)dx_0, \tag{2.1}$$

where $\rho(x_0)$ is the diagonal element of the density matrix

$$\rho(x_0)=\langle x_0|\exp(-\beta H)|x_0\rangle \tag{2.2}$$

and H is the Hamiltonian. The cyclic property of the closed chain allows the standard unnormalized density $\rho(x_0)$ to be expressed as

$$\rho(x_0)=\int_{x(0)}^{x(1)=x(0)}[\mathscr{D}x(u)]\int_0^1 du\,\delta[x(u)-x_0]\exp-S \tag{2.3}$$

in which S is the dimensionless Euclidian action given by

$$S=\frac{m}{2\hbar^2\beta}\int_0^1\left(\frac{\partial x}{\partial u}\right)^2 du+\beta\int_0^1 V[x(u)]du, \tag{2.4}$$

where the discretized form of the measure $[\mathscr{D}x(u)]$ is explicitly given by

$$[\mathscr{D}x(u)]=\lim_{p\to\infty}\left(\frac{mP}{2\pi\beta\hbar}\right)^{p/2}\prod_{k=1}^{P}dx_k \tag{2.5}$$

for P beads. This differs slightly from the standard form of the measure which does not have the integral of dx_P.

The canonical partition function can also be expressed as

$$Z=\int \rho^*(x_0)dx_0 \tag{2.6}$$

with $\rho^*(x_0)$, the unnormalized centroid density, defined as

$$\rho^*(x_0)=\int_{x(0)}^{x(1)=x(0)}[\mathscr{D}x(u)]\delta(\bar{x}-x_0)\exp-S, \tag{2.7}$$

where the measure $[\mathscr{D}x(u)]$ is also given by Eq. (2.3) and $\bar{x}$ is the centroid (or the center-of-mass) of the closed chain

$$\bar{x}=\int_0^1 x(u)du. \tag{2.8}$$

ρ in Eq. (2.3) involves a sum over all the paths which pass through the point x_0, while ρ^* in Eq. (2.7) involves the sum over all paths whose center-of-mass is located at x_0. Feynman[2] used the concept of the centroid density to derive a quantum correction to the partion function.

In the following, we shall omit the term "unnormalized" because both the standard density of Eq. (2.3) and the centroid density of Eq. (2.7) are normalized by the partition function Z.

It is often useful to choose an exactly soluable reference system with potential funtion $V_{\rm ref}$ and to express the centroid density for the real system in terms of the centroid density for the reference system $\rho^*_{\rm ref}(x_0)$. In general,

$$\rho^*(x_0)=\rho^*_{\rm ref}(x_0)\langle\exp-\beta\int(V-V_{\rm ref})du\rangle_{\rm ref}, \tag{2.9}$$

where $\langle\cdots\rangle_{\rm ref}$ is the average (or the expectation value) in the reference system

$$\langle f\rangle_{\rm ref}=\frac{\int[\mathscr{D}x(u)]\delta(\bar{x}-x_0)f(x)\exp-S_{\rm ref}}{\int[\mathscr{D}x(u)]\delta(\bar{x}-x_0)\exp-S_{\rm ref}}. \tag{2.10}$$

In principle, any reference system can be employed to evaluate the centroid density corresponding to another potential, but convergence is best for a reference system physically close to the system of interest. The two reference systems treated in this paper are the free particle and linear harmonic oscillator reference systems.

B. The cumulant expansion

In this section, we apply a cumulant expansion to average over a free particle reference system ($V_{\rm ref}=0$) to obtain an effective potential as a power series expansion in powers of the inverse temperature.

The path can be expanded in a Fourier series

$$x(u)=x_0+\sum_{k=1}^{\infty}[a_k\cos(2\pi ku)+b_k\sin(2\pi ku)] \tag{2.11}$$

which automatically satisfies the constraint that the centroid of the path must be located at x_0[cf. Eq. (2.8)] as well as the requirement that the closed chain be periodic over the interval $u=0$ to $u=1$. Substitution of this Fourier series into Eq. (2.4) for a free particle gives the action

$$S_{\rm ref}=\sum_{k=1}^{\infty}\frac{a_k^2+b_k^2}{2\sigma_k^2}, \tag{2.12}$$

where σ_k is the thermal wavelength of the k th mode

$$\sigma_k^2=\hbar^2\beta/2\pi mk^2. \tag{2.13}$$

The average defined in Eq. (2.10) can be expressed as an infinite dimensional Gaussian integral

$$\langle f\rangle_{\rm ref}=\frac{\prod_{k=1}^{\infty}\int da_k\,db_k f e^{-(a_k^2+b_k^2/2\sigma_k^2)}}{\prod_{k=1}^{\infty}(2\pi\sigma_k^2)} \tag{2.14}$$

and σ_k can also be viewed as the Gaussian width of each mode.

As is well known, averages of $\exp[-f(x)]$ can be written as a cumulant expansion,[11]

$$\left\langle\exp\left[-\beta\int_0^1 V[x(u)]du\right]\right\rangle_{\rm ref}=\exp\left[\sum_{m=1}^{\infty}\frac{(-\beta)^m}{m!}C_m\right]$$
$$=\exp[-\beta V_{\rm eff}], \tag{2.15}$$

where C_m is mth order cumulant which is related to the moments

$$I_m=\left\langle\left\{\int_0^1 du\,V[x(u)]\right\}^m\right\rangle_{\rm ref}. \tag{2.16}$$

The first few cumulants are

$$C_1=I_1, \tag{2.17}$$

$$C_2=I_2-I_1^2, \tag{2.18}$$

$$C_3=I_3-3I_1I_2+2I_1^3. \tag{2.19}$$

For C_1, the multidimensional Gaussian averge over a_k and b_k is easily evaluated by first expressing $V[x(u)]=V[x_0+\tilde{x}(u)]$, where $\tilde{x}(u)\equiv x(u)-x_0$, as a Fourier transform. This reduces to a Gaussian average over a single variable $\tilde{x}$:

$$C_1=\left\langle\int V(x_0+\tilde{x})du\right\rangle_{\sigma}$$
$$=\frac{1}{\sqrt{2\pi\sigma^2}}\int d\tilde{x}\,V(x_0+\tilde{x})\exp-[\tilde{x}^2/2\sigma^2] \tag{2.20}$$

with the Gaussian width

$$\sigma^2=\sum_{k=1}^{\infty}\sigma_k^2[\cos^2(2\pi ku)+\sin^2(2\pi ku)]=\frac{\hbar^2\beta}{12m}, \tag{2.21}$$

where the summation $\Sigma_{k=1}^{\infty}(1/k^2)=\pi/6$ was explicitly used, σ can be understood as the thermal wavelength of a free particle. By Taylor expanding $V(x_0+\tilde{x})$ in Eq. (2.20) around x_0, and by evaluating the Gaussian integrals of $\tilde{x}^n$, C_1 can be expressed as a power series expansion in β, $(\sigma^2\sim\beta)$,

$$C_1=\sum_n\frac{(2n-1)!!}{(2n)!}V^{(2n)}(x_0)(\sigma^2)^n, \tag{2.22}$$

where $V^{(2n)}(x_0)=d^{2n}V(x_0)/dx_0^{2n}$. There are no such simple solutions for higher order cumulants. To proceed the potential is Taylor expanded and the result is integrated term by term over u before evaluating the average

$$\int V(x_0+\tilde{x})du=\sum_{n=1}^{\infty}\frac{1}{(2n)!}V^{(2n)}(x_0)\int du\,\tilde{x}(u)^{2n}. \tag{2.23}$$

The odd terms vanish when integrated over u and the moment I_2 in Eq. (2.42) is explicitly given by

$$I_2=\int du\int du'\langle V[x(u)]V[x(u')]\rangle_{\rm ref}. \tag{2.24}$$

Substitution of Eqs. (2.24) and (2.20) into Eq. (2.19) yields the leading term of C_2 to order β^2,

$$C_2=\left[\frac{V^{(2)}}{2!}\right]^2\sum_{k=1}^{\infty}\sigma_k^4+O(\beta^3)=\frac{[V^{(2)}]^2}{10}\sigma^4+O(\beta^3), \tag{2.25}$$

where the sum $\Sigma_{k=1}^{\infty}(1/k^4)=\pi^2/90$ has been explicitly used.

Proceeding in this manner, it is easy to show that the third order cumulant

$$C_3=(I_3-I_1^3)-3I_1C_2 \tag{2.26}$$

is also in order of β^2, because $(I_3-I_1^3)\sim O(\beta^3)$; i.e., $C_3\sim O(\beta^2)$.

Finally, using the foregoing, it follows that the quantum corrections to the unnormalized centroid density to the fourth order of β can be expressed as

$$\rho^*(x_0)=\sqrt{\frac{m}{2\pi\hbar^2\beta}}\exp-(\beta V_{\rm eff}) \tag{2.27}$$

with effective potential

$$V_{\rm eff}=V+\frac{V^{(2)}}{2}\sigma^2+\frac{V^{(4)}}{8}\sigma^4+\frac{V^{(6)}}{48}\sigma^6$$
$$-\beta\frac{(V^{(2)})^2}{20}\sigma^4+O(\beta^4). \tag{2.28}$$

It should be noted that no odd derivatives of the potential appear in the effective potential. This is different from the standard density Eq. (2.3) which includes force terms in the high order expansion, i.e., the well-known Wigner expansion.[12]

Application of the above to the linear harmonic oscillator (LHO), $V=m\omega^2x^2/2$, gives

$$\beta V_{\rm eff}\simeq\beta V+\frac{\alpha^2}{24}-\frac{\alpha^4}{2880}, \tag{2.29}$$

where $\alpha=\beta\hbar\omega$, a result in very good agreement with the first few terms of the exact result [cf. Eq. (A5)].

From $E=-\partial\ln Z/\partial\beta$, it is easy to determine that

$$E=\frac{1}{2\beta}+\left\langle V+V^{(2)}\sigma^2+\frac{3V^{(4)}}{8}\sigma^4+\frac{V^{(6)}}{12}\sigma^6\right.$$
$$\left.-\beta\frac{(V^{(2)})^2}{5}\sigma^4\right\rangle_{\rho^*}, \tag{2.30}$$

where $\langle\cdots\rangle$ indicates the ensemble average of distribution

ρ^*, a result that defines the energy estimator ϵ as the unaveraged quantity

$$\epsilon = \frac{1}{2\beta} + V + V^{(2)}\sigma^2 + \frac{3V^{(4)}}{8}\sigma^4 + \frac{V^{(6)}}{12}\sigma^6 - \beta\frac{(V^{(2)})^2}{5}\sigma^4. \tag{2.31}$$

We call this method the effective potential approximation in the free particle reference system (EPFRS approximation).

The above results can be generalized to a three-dimension particle simply by substituting $V^{(2n)}$ with $\Sigma_{i=1}^{3}\partial_i^{(2n)}V$ and the constant $1/2\beta$ in the energy estimator is replaced by $3/2\beta$.

C. The effective frequency from a harmonic reference system

The low temperature propagator [Eq. (1.3)] introduced by Mak and Andersen requires an explicit effective frequency. Mak and Andersen give two *ad hoc* prescriptions for determining ω [cf. Eqs. (1.5) and (1.6)]. In this section, we introduce another method for determining ω and in the next section we show that the short time propagator using this prescription is superior to that of Mak and Andersen.

Our method is based on the early work of Feynman[9] who used the centroid density to determine an effective classical partition function. Gillan[13] derived an expression for quantum transition state theory by replacing the classical density $\rho_{\rm cl}$ at the top of the barrier by the corresponding centroid density $\rho^*(x_0)$. Voth *et al.*[10] developed an approximation for ρ^* in a metastable system using a variation principle, determined an effective frequency for the parabolic barrier, and applied the result as an importance sampling function in real-time barrier crossing dynamics simulations. Based on the foregoing work, we are able to formulate a simple expression for the effective frequency to be used in the low temperature propagator and to calculate the energy of a quantum system to a very good approximation.

The reference system is chosen to be the linear harmonic reference system with potential

$$V_{\rm ref} = V(x_0) + \tfrac{1}{2}m\omega^2(\tilde{x})^2, \tag{2.32}$$

where the unspecified parameter ω is the effective frequency—to be determined.

The well-known inequality $\langle \exp(-f)\rangle \geqslant \exp(-\langle f\rangle)$ allows one to derive the inequality

$$\left\langle \exp -\beta\int (V - V_{\rm ref})du \right\rangle_{\rm ref} \geqslant \exp -\beta\left\langle \int (V - V_{\rm ref})du \right\rangle_{\rm ref}, \tag{2.33}$$

where $\langle\cdots\rangle_{\rm ref}$ is defined in Eq. (2.10). Thus, substitution of this into Eq. (2.9) yields

$$\rho^*(x_0) \geqslant \rho^*_{\rm ref}(x_0)\exp -\beta\left\langle \int (V - V_{\rm ref})du \right\rangle_{\rm ref}. \tag{2.34}$$

The effective frequency is found by maximizing the term on the right-hand side of Eq. (2.34) at each point x_0. This variation procedure gives (see the Appendix)

$$m\omega^2 = \langle V''(x_0 + \tilde{x})\rangle_\sigma, \tag{2.35}$$

where $\langle\cdots\rangle_\sigma$ is the Gaussian average

$$\langle V''(x_0 + \tilde{x})\rangle_\sigma = \left[\frac{1}{\sqrt{2\pi\sigma^2}}\right]\int d\tilde{x}\, V''(x_0 + \tilde{x}) \times \exp[-\tilde{x}^2/2\sigma^2] \tag{2.36}$$

and the Gaussian width defined as

$$\sigma^2 = \frac{\hbar^2\beta}{m\alpha^2}\left[\frac{\alpha/2}{\tanh(\alpha/2)} - 1\right], \tag{2.37}$$

where $\alpha = \beta\hbar\omega$.

In the Appendix it is shown that for a metastable barrier, the corresponding equation for the effective frequency of the barrier reduces to the results of Voth *et al.*[10]

It is important to note that both sides of Eq. (2.35) depend on ω and the resulting transcendental equation must be solved for ω. Expansion about the centroid point x_0 yields another form of Eq. (2.35) which is more practical for solving for ω:

$$m\omega^2 = \sum_{n=0}^{\infty}\frac{(2n-1)!!}{(2n)!}V^{(2n+2)}(x_0)\sigma^{2n}. \tag{2.38}$$

Equation (2.37) can also be expanded to give

$$\sigma^2 = \sigma_0^2\left[1 - \frac{1}{15}\left(\frac{\alpha}{2}\right)^2 + \frac{2}{315}\left(\frac{\alpha}{2}\right)^4 + \cdots\right], \tag{2.39}$$

where $\sigma_0^2 = \hbar^2\beta/12m$ and $\alpha = \beta\hbar\omega$.

Substitution of Eq. (2.39) into Eq. (2.38) leads to a perturbation series for ω^2 in terms of β. The first few terms are

$$m\omega^2 = V^{(2)} + \frac{V^{(4)}}{2}\sigma_0^2 + \frac{V^{(6)}}{8}\sigma_0^4\frac{V^{(8)}}{48}\sigma_0^6 - \beta\frac{V^{(2)}V^{(4)}}{10}\sigma_0^4 + O(\beta^4). \tag{2.40}$$

Note that the second derivative of Eq. (2.28) gives the same result. This illustrates the relationship between the cumulant expansion using a free particle reference system and the variational approach based on the harmonic oscillator reference system. Thus, these two approximations are equivalent in the limit of high temperature. In the low temperature limit, on the one hand, it is possible to include higher order cumulants. On the other hand, the effective frequency approach is a very accurate approximation if the anharmonicity in the potential is not too large.

As has already been pointed out, the centroid density depends only on even derivatives of the potential, whereas the semiclassical expansion of the diagonal density matrix depends on even and odd derivatives of the potential. Therefore, the quadratic reference potential is a good starting point for calculations involving the centroid density, whereas for the standard density defined in Eq. (2.3), a forced harmonic potential must be used in order to include the first two terms in the expansion.

In general, the effective frequency ω given by Eq. (2.35) is not related to the local curvature, but involves an average over a Gaussian width σ defined by Eq. (2.37), which can be

interpreted as the thermal wavelength of a particle in the reference LHO potential. Essentially, σ reveals all the quantum effects in the reference potential. In the limit of $\alpha \to 0$, σ reduces to the free particle thermal wavelength $\sigma_0^2 = \hbar^2\beta/12m$.

The foregoing suggests that the effective frequency ω to be used in the low temperature propagator [Eq. (1.4)] be taken as the solution of Eq. (2.35) at the minimum of the potential. This choice has the advantage that the self-consistent equation for ω contains accurate information about quantum effects in the ground state. We call this modified propagator the effective frequency low temperature (EFLT) propagator.

In multiple well problems the centroid can move from one well to another. In this case the effective frequency is variable and corresponds to the minimum of the potential well in which the centroid is located at each time.

The right-hand side of inequality (2.10) with the optimized choice for the effective frequency gives a useful approximation to the exact centroid density, which we label $\tilde{\rho}^*$,

$$\tilde{\rho}^*(x_0) = \sqrt{\frac{m}{2\pi\hbar^2\beta}}\frac{\alpha/2}{\sinh(\alpha/2)}\exp -\beta\left(\langle V(x_0+\tilde{x})\rangle_\sigma - \frac{m\omega^2}{2}\sigma^2\right), \tag{2.41}$$

where ω is a function of position x_0 defined by Eq. (2.35), and thus depends on β, $\hbar$, and mass. This generates an approximation for the partition function $Z \simeq \int \tilde{\rho}^*(x_0)dx_0$. Substitution of this into $E = -\partial \ln Z/\partial\beta$ allows us to determine the average energy as [see Eq. (B10)]

$$E = \left\langle \frac{\hbar\omega}{4}\operatorname{cth}(\alpha/2) + \langle V(x_0+\tilde{x})\rangle_\sigma \right\rangle_{\tilde{\rho}^*}, \tag{2.42}$$

where $\langle V(x_0+\tilde{x})\rangle_\sigma$ is defined by Eqs. (2.36) and (2.37) and $\langle\cdots\rangle_{\tilde{\rho}^*}$ indicates the average over the classical distribution function $\tilde{\rho}^*$. As this method is based on the local effective quadratic reference potential, we call it the effective quadratic potential (EPQRS) approximation. Equation (2.42) permits us to define the energy estimator for this approximation as

$$\epsilon = \frac{\hbar\omega}{4}\operatorname{cth}(\alpha/2) + \langle V(x_0+\tilde{x})\rangle_\sigma. \tag{2.43}$$

This must be averaged over the distribution function $\tilde{\rho}^*$.

Application of these results to the trivial problem of a LHO using the harmonic reference system leads to ω = constant and the energy estimator gives the exact results.

$$E = \frac{\hbar\omega}{2}\operatorname{cth}(\alpha/2). \tag{2.44}$$

It is a simple matter to construct a Monte Carlo algorithm based on umbrella sampling[1,14] in which the configuration is sampled according to the true classical distribution $\exp(-\beta V)$, where V is the full potential and any quality to be averaged is weighed by the difference between the classical and the approximated centroid density, i.e., $\tilde{\rho}^*/\rho_{\rm cl}$.

The above results can be easily generalized to multidimensional systems. If the vector $\mathbf{x}$ denotes the set of N coordinates $\{x_1, x_2, \ldots, x_n\}$, there will be a corresponding $N \times N$ matrix of frequencies, ω_{ij}^2. With the help of the transform matrix R, we can diagonize the frequency matrix,

$$R^T\omega^2 R = \omega'^2. \tag{2.45}$$

The Gaussian width σ is defined similarly to Eq. (2.37), where the frequency ω will be replaced by the eigenvalues of the frequency matrix $\{\omega_1'^2, \ldots, \omega_n'^2\}$. For each eigenfrequency, we have

$$\sigma'^2 = \frac{\hbar^2\beta}{m\alpha'^2}\left(\frac{\alpha'/2}{\tanh(\alpha'/2)} - 1\right), \tag{2.46}$$

where $\alpha_i' = \hbar\beta\omega_i'$. Obviously, the Gaussian averages are taken with the transformed coordinates $\bar{x}$ 'which are related to $\bar{x}$ by the rotation matrix $\tilde{x}_i = R_{ij}\tilde{x}_j'$. The Gaussian average can then be formulated in terms of x',

$$\langle F(\mathbf{x}_0+\tilde{x})\rangle_{\sigma'} = \prod_{i=1}^{n}\left[\frac{1}{\sqrt{2\pi\sigma_i'^2}}\int dx_i' \exp\frac{-x_i'^2}{2\sigma_i'^2}\right] \times F(\mathbf{x}_0 + R\tilde{x}'). \tag{2.47}$$

It is then straightforward to generalize Eq. (2.35), which now reads

$$m\omega_{ij}^2 = \langle \partial_i\partial_j V(\mathbf{x}_0+\tilde{x})\rangle_{\sigma'}. \tag{2.48}$$

It should be noted that the transformation of coordinates is local as the rotation matrix depends on the effective frequency matrix which varies with position. If interactions between different groups of coordinates are weakly coupled, $\mathbf{x}$ can be divided into several essentially independent subsets of coordinates and the computation of the N-dimensional centroid will be significantly simplified.

III. RESULTS

For simplicity, we assign a number, a symbol, and an acronym to denote the different approximations introduced previously:

(1) □ (HT propagator), the standard high temperature propagator [Eq. (1.1)].

(2) ○ (LT propagator), the low temperature propagator [Eqs. (1.3) and (1.6)].

(3) △ (EFLT propagator), the effective frequency low temperature propagator [Eqs. (1.3) and (2.35)].

(4) ⋆ (EPQRS approximation), the effective potential approximation using the quadratic reference system [Eqs. (2.35), (2.41), and (2.42)].

(5) ⊕ (EPFRS approximation), the high order effective potential expansion [Eqs. (2.27), (2.28), and (2.30)].

Methods (1)–(3) are employed to calculate the short time propagator to be used in path integral Monte Carlo simulations and the virial estimator[15] is used to calculate the average energy. The number of moving beads P used in the staging algorithm is adjusted to yield an acceptance rate of approximately 50%. The results are based on MC simulations of 10^5 passes. The dotted line in the figures are the converged values as described below. In all cases, $m = 1.0$ and $\hbar = 1.0$. Mak *et al.* have already shown[8] that the LT propagator converges faster than the HT propagator.

Methods (4) and (5) are two approximations to the

centroid density which can be used to determine the energy by numerically evaluating the spatial integration in Eq. (2.30) or Eq. (2.42).

We investigate these five methods using a simple anharmonic potential for which the energy eigenvalues can be analytically evaluated. For a three-dimensional isotropic harmonic oscillator of frequency $\omega = 1.0$, with the angular momentum quantum number $L = 1$, the effective radial potential is

$$V = \frac{x^2}{2} + \frac{1}{x^2}. \tag{3.1}$$

For this potential, the ground state energy is $\frac{3}{2}\hbar\omega$ and the energy levels are $E_n = (\frac{3}{2} + 2n)\hbar\omega$. The average energy of this system at temperature β is given by

$$E = \frac{3}{2} + \frac{2}{e^{2\beta} - 1} \tag{3.2}$$

for units in which $\hbar = 1.0$ and $\omega = 1.0$.

Figure 1 gives the average energy vs β using the five different methods listed above. The dotted line is the exact energy calculated from Eq. (3.2). The path integral staging Monte Carlo simulation is performed with three propagators [(1), (2), and (3)], respectively, with the same number of beads at each temperature. The number of beads P varies from two to five at different β. The plots clearly show that the EFLT propagator [method (3)] is superior to the others, as we expected.

The EPQRS approximation [method (4)] with the expansion of $\langle V \rangle$ and $\langle V'' \rangle$ carried out to the sixth order in the derivatives of the potential $V^{(6)}$, clearly gives the better agreement with the exact result than does the EPFRS approximation [method (5)]. It works well even at low temperature, whereas the EPFRS approximation works reasonably well at high temperature and poorly at low temperatures.

In order to study the convergence with P and to investigate the behavior as the strength of the anharmonicity varies, it is useful to investigate the quartic potential

$$V = \frac{x^2}{2} + \lambda x^4, \tag{3.3}$$

where λ gives the strength of anharmonicity.

Figure 2, a plot of the effective frequency ω [cf. Eq. (2.35)] vs β at the minimum point $x = 0$, for $\lambda = 1$, clearly shows that in the high temperature limit (classical limit) the effective frequency ω approaches the local curvature at the potential minimum (with corresponding frequency = 1.0) calculated from Eq. (1.5). In the low temperature limit ($\beta \to \infty$), the Gaussian width σ, defined by Eq. (2.37), becomes

$$\sigma^2 = \frac{\hbar}{2m\omega} \tag{3.4}$$

which is independent of β for any $\omega > 0$. $\sigma = \sqrt{\hbar/2m\omega}$ is actually the spatial spread of the ground state of a linear harmonic oscillator of frequency ω. Thus for the quartic potential [Eq. (3.3), it follows from Eq. (2.38) that

$$m\omega^2 = 1 + 12\lambda x^2 + 12\lambda \frac{\hbar}{2m\omega}, \tag{3.5}$$

which gives the effective frequency in the $\beta \to \infty$ limit. Solving Eq. (3.5) for ω, allows us to compute the ground state energy of the quartic potential by evaluating the ground state energy of the corresponding effective quadratic potential $\hbar\omega/2$. For comparison, Eq. (1.6) gives $\omega_{\text{nor}} = 1.53$, which lies between the high and low temperature limits.

In Fig. 3, we plot the effective frequency corresponding to the quartic potential [Eq. (3.3)] with $\lambda = 1$, as a function of position x_0 for fixed temperature $\beta = 5.0$. Curve (a) gives the Gaussian width $\sigma(\times 10)$ defined by Eq. (2.37). Curve

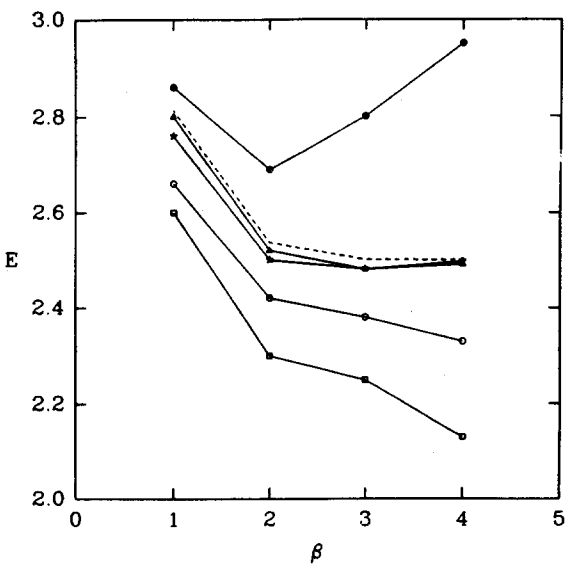

FIG. 1. A plot of average energy vs β. The potential is defined by Eq. (3.1) The dotted line is the exact results obtained from Eq. (3.2). (1) □ indicates the data for HT propagator; (2) ○ indicates the data for LT propagator; (3) △ indicates the data for EFLT propagator. The above three propagators are employed in staging MC simulation with the same number of beads. (4) * is the results of EPQRS approximation; and (5) ⊕ is the results of EPFRS approximation.

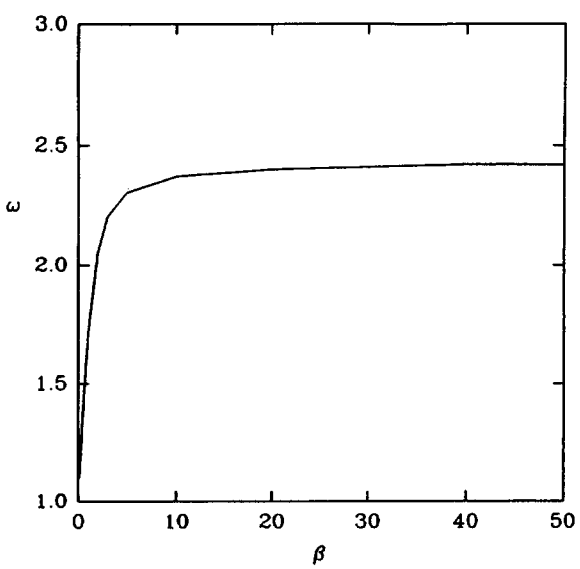

FIG. 2. The effective frequency determined by Eq. (2.35) for a quartic potential [Eq. (3.3)] with $\lambda = 1$ at $x = 0$ is plotted vs β.

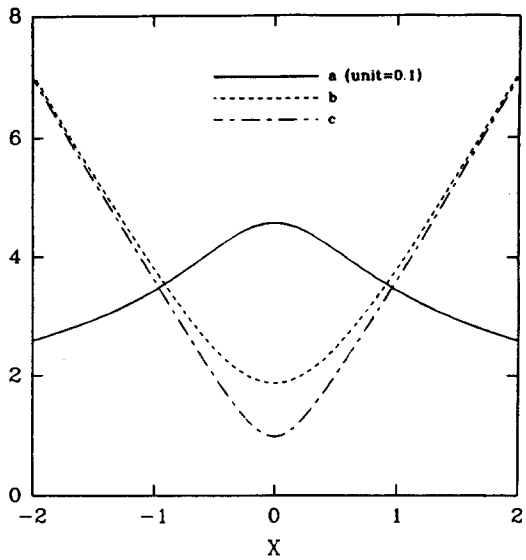

FIG. 3. A plot of the effective frequency as a function of position at $\beta = 5$. The same potential as in Fig. 2 is used. Curve (a) is the Gaussian width σ defined in Eq. (2.37); curve (b) is the effective frequency; curve (c) is the local curvature frequency [Eq. (1.5)].

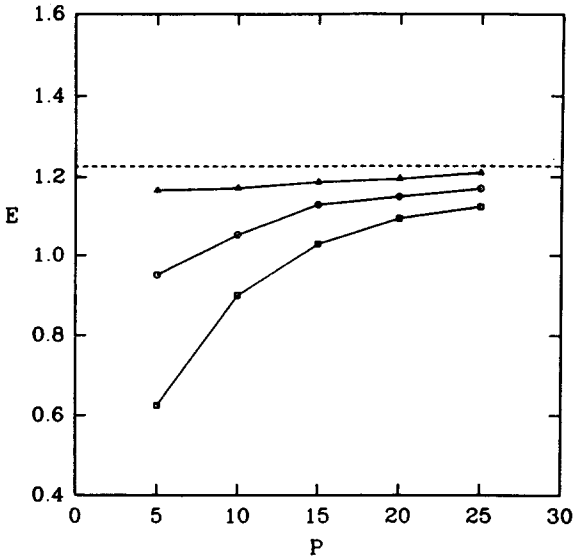

FIG. 5. The same plot as Fig. 4 except for a different parameter $\lambda = 5$.

(b) corresponds to the effective frequency solved from Eq. (2.35) and curve (c) corresponds the local curvature frequency determined by Eq. (1.5). These curves show that the quantum effect is largest at $x = 0$.

Next we study how the energy of the quartic oscillator [Eq. (3.3)] converges as a function of the number of beads P used in the staging Monte Carlo method for the three propagators (1), (2), and (3). In Fig. 4, $\lambda = 1.0$ and $\beta = 5.0$, whereas in Fig. 5, $\lambda = 5.0$ and $\beta = 5.0$. These are compared with the exact energies determined from the paper of Zhang *et al.*[7] using the basis set for the LHO. Figures 4 and 5 clearly show that the EFLT propagator [method (3)] converges more rapidly than the LT propagator [method (2)], which in turn converges more rapidly than the HT propagator [method (1)]. Because the EFLT [method (2)] and the LT [method (3)] propagators are based on a quadratic aproximation, we expect them to be excellent when the anharmonicity λ is small. Comparison of Figs. 4 ($\lambda = 1.0$) and 5 ($\lambda = 5.0$) shows that these two methods [(2) and (3)] for any given P are closer to the exact result for $\lambda = 1.0$ than for $\lambda = 5.0$. The EPQRS approximation [method (4)] is also applied to both cases and the results are listed in Table I.

Finally, it is of interest to see if our conclusions also apply to multidimensional potentials. For this purpose we study the simple two-dimensional potential,

$$V(x,y) = V_1(x) + V_1(y) + V_2(x,y), \tag{3.6}$$

where the V_1's are one body potentials and V_2 is the coupling potential

$$V_1(x) = 5x^4 + \tfrac{1}{2}x^2, \tag{3.7}$$

$$V_1(y) = 5y^4 + \tfrac{1}{2}y^2, \tag{3.8}$$

$$V_2(x,y) = xy. \tag{3.9}$$

For $\beta = 5.0$, $\hbar = 1.0$, and $m = 1.0$, the frequency ma-

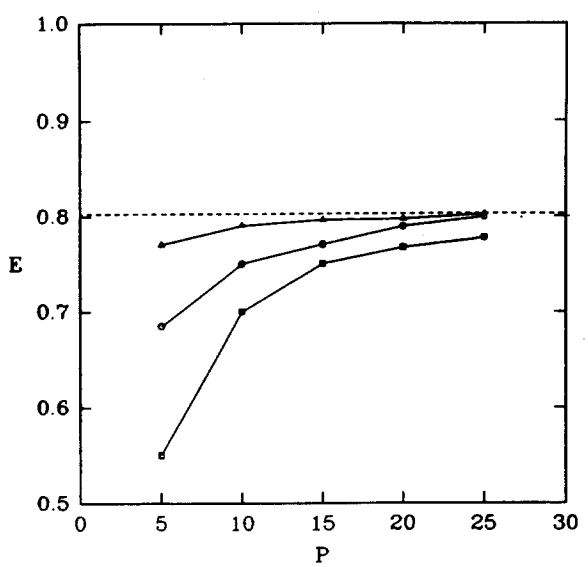

FIG. 4. A plot of average energy of the quartic potential ($\lambda = 1$) the number of beads P in the staging MC simulation. $\beta = 5$. The results are indicated by (1) □ for the HT propagator, (2) ○ for the LT propagator, (3) △ for the EFLT propagator. The number of MC passes is 10^5. And the acceptance rate is adjusted to approximate 50%.

TABLE I. Energy comparison. λ is the parameter in the quartic potential defined by Eq. (3.3). E_{exact} is calculated with the help of the basis set of LHO. E_{weff} is the result of EPQRS approximation. ω_{weff} is the solution to Eq. (2.35) to be used in EFLT propagator. ω_{nor} is the solution to Eq. (1.6) to be used in LT propagator.

λ	E_{exact}	E_{weff}	ω_{weff}	ω_{nor}
1	0.803	0.787	1.88	1.53
5	1.226	1.218	3.08	2.29

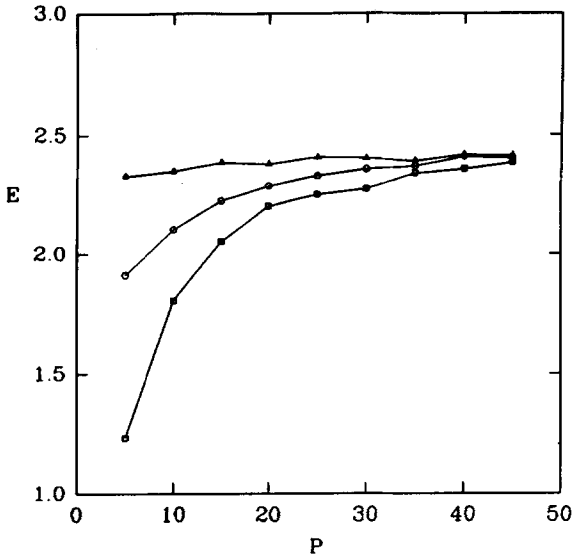

FIG. 6. Average energy for a two-dimensional potential defined in Eq. (3.6) at $\beta = 5$ is plotted vs the number of heads used in the staging algorithm. The results are indicated by (1) □ for the HT propagator, (2) ○ for the LT propagator, (3) △ for the EFLT propagator. The number of MC passes is 10^5. And the acceptance rate is adjusted to approximate 50%.

trix of method (2) is $\omega^2 = \left(\begin{smallmatrix} 5.2 & 1.0 \\ 1.0 & 5.2 \end{smallmatrix}\right)$ and that of method (3) is $\omega^2 = \left(\begin{smallmatrix} 9.5 & 1.0 \\ 1.0 & 9.5 \end{smallmatrix}\right)$.

For details concerning the treatment of this multidimensional potential using the low temperature propagator approximation, we refer the reader to the paper by Mak *et al.*[8] In Fig. 6, we show a plot of the average energy vs the number of beads P. For this two-dimensional case, we have not determined the exact energy and, consequently, we do not include a dotted curve for comparison. Nevertheless, it is clear from Fig. 6 that our EFLT propagator for this two-dimensional potential retains its superiority over the other alternatives.

ACKNOWLEDGMENT

This work was supported by a grant from the NSF.

APPENDIX A: THE FREE PARTICLE REFERENCE SYSTEM

The exact form of the centroid density of the LHO potential defined by Eq. (2.32) is now derived. The Fourier transformation defined by Eq. (2.11) gives the action

$$S = V(x_0) + \sum_{k=1}^{\infty} \frac{a_k^2 + b_k^2}{2\sigma_k^2}, \tag{A1}$$

where σ_k is given by

$$\sigma_k^2 = \frac{\hbar^2\beta}{2m\pi^2} \frac{1}{k^2 + (\alpha/2\pi)^2} \tag{A2}$$

which reduces to the free particle result as $\alpha \to 0$.

Substitution of the identity

$$\prod_{k=1}^{\infty} \frac{1}{1 + (\alpha/2\pi k)^2} = \frac{\alpha/2}{\sinh(\alpha/2)} \tag{A3}$$

gives the results

$$\rho^*(x_0) = \sqrt{\frac{m}{2\pi\hbar^2\beta}} \frac{\alpha/2}{\sinh(\alpha/2)} \exp -\beta V(x_0) \tag{A4}$$

which for small α can be expanded as

$$\rho^*(x_0) = \sqrt{\frac{m}{2\pi\hbar^2\beta}} \exp -\left(\beta V + \frac{\alpha^2}{24} - \frac{\alpha^4}{2880} + \cdots\right). \tag{A5}$$

APPENDIX B: THE HARMONIC REFERENCE SYSTEM

To apply Eq. (2.34), we require the calculation of $\langle V(x_0 + \tilde{x}(u))\rangle_{\text{ref}}$. To proceed, we substitute Eq. (2.11) for $\tilde{x}(u)$ and evaluate Eq. (2.14). It is easy to show that

$$\langle V[x_0 + \tilde{x}(u)]\rangle_{\text{ref}} = \langle V(x_0 + \tilde{x})\rangle_{\sigma}, \tag{B6}$$

where $\langle\cdots\rangle_{\text{ref}}$ is defined by Eq. (2.14) and $\langle\cdots\rangle_{\sigma}$ is defined by Eq. (2.20). The Gaussian width σ is given by

$$\sigma^2 = \sum \sigma_k^2, \tag{B7}$$

where σ_k has already been defined by Eq. (A2). After substituting the following identity

$$\sum_{k=1}^{\infty} \frac{1}{k^2 + y^2} = \frac{1}{2}\left[\frac{\pi}{y}\,\text{cth}\,(\pi y) - \frac{1}{y^2}\right] \tag{B8}$$

into Eq. (B7), we recover Eq. (2.37).

The variation principle applied to the right-hand side of Eq. (2.34) yields

$$\left.\frac{\partial}{\partial\omega}\tilde{\rho}^*\right|_{\beta} = \hbar\beta + \left.\frac{\partial}{\partial\alpha}\tilde{\rho}^*\right|_{\beta} = 0, \tag{B9}$$

where the explicit form of $\tilde{\rho}^*$ is given by Eq. (2.41). Equation (2.35) is the solution of Eq. (B9).

To derive the energy estimator (2.42), we evaluate the partial derivative of $\tilde{\rho}^*$ with respect to β:

$$\left.\frac{\partial}{\partial\beta}\tilde{\rho}^*\right|_{\omega} = \left.\frac{\partial}{\partial\beta}\tilde{\rho}^*\right|_{\alpha} + \left.\frac{\partial\alpha}{\partial\beta}\frac{\partial}{\partial\alpha}\tilde{\rho}^*\right|_{\beta} = \left.\frac{\partial}{\partial\beta}\tilde{\rho}^*\right|_{\alpha}, \tag{B10}$$

where we drop the term involving the partial derivative with respect to α because of Eq. (B9). Then, Eq. (2.42) is easily obtained.

APPENDIX C: THE PARABOLIC REFERENCE SYSTEM

Finally, for a parabolic reference potential

$$V_{\text{ref}} = V(x_0) - \tfrac{1}{2}m\omega_b^2(x - x_0)^2, \tag{C11}$$

we simply redefine the variable $\omega = i\omega_b$, $\alpha = i\alpha_b$. Then Eqs. (2.35) and (2.37) reduce to

$$m\omega_b^2 = -\langle V''(x_0 + \tilde{x})\rangle_{\sigma}, \tag{C12}$$

where σ is given by

$$\sigma^2 = \frac{\hbar^2\beta}{m\alpha_b^2}\left(1 - \frac{\alpha_b/2}{\tan\alpha_b/2}\right). \tag{C13}$$

There exists an upper bound for the effective barrier frequency $\alpha_b \leqslant 2\pi$, because σ diverges when $\alpha_b = 2\pi$.

The transcendental equation for ω given by Voth *et al.*[10] is

$$m\omega_b^2 = \int_{\infty}^{\infty} \frac{dk}{2\pi} k^2 \tilde{V}(k) \exp(ikx_0 - k^2 \Delta q^2/2), \quad \text{(C14)}$$

where Δq^2 is the mean-square deviation from the centroid

$$\Delta q^2 = \int_0^1 \langle [x(u) - x_0]^2 \rangle_{\text{ref}} \, du. \quad \text{(C15)}$$

It is easy to verify that Δq^2 is exactly the Gaussian width σ^2 we give in Eq. (C13).

$\tilde{V}(k)$ is the Fourier transformation of the potential V:

$$\tilde{V}(k) = \int_{\infty}^{\infty} V(x) \exp(-ikx) dx. \quad \text{(C16)}$$

Substitution of Eq. (C16) into Eq. (C14) followed by the integration over k yields our previous result Eq. (C12). Therefore, we have verified the equivalency of Eqs. (C14) and (2.35).

[1] B. J. Berne and D. Thirumalai, Annu. Rev. Phys. Chem. **37**, 401 (1986). For references on path integral Monte Carlo, see the papers cited here.
[2] R. P. Feynman and A. R. Hibbs, *Quantum Mechanics and Path Integrals* (McGraw-Hill, New York, 1965).
[3] L. S. Schulman, *Techniques and Applications of Path Integrals* (Wiley, New York, 1986).
[4] J. A. Barker, J. Chem. Phys. **70**, 2914 (1979).
[5] M. Suzuki, Commun. Math. Phys. **51**, 183 (1976).
[6] N. Makri and W. H. Miller, J. Chem. Phys. **90**, 904 (1989).
[7] P. Zhang, R. M. Levy, and R. A. Friesner, Chem. Phys. Lett. **144**, 236 (1988).
[8] C. H. Mak and H. C. Andersen, J. Chem. Phys. **92**, 2953 (1990).
[9] R. P. Feynman and H. Kleinert, Phys. Rev. A. **34**, 5080 (1986).
[10] G. A. Voth, D. Chandler, and W. H. Miller, J. Chem. Phys. **91**, 7749 (1989).
[11] R. D. Coalson, D. L. Freeman, and J. D. Doll, J.Chem. Phys. **91**, 4242 (1989).
[12] E. P. Wigner, Phys. Rev. **40**, 749 (1932).
[13] M. J. Gillan, J. Phys. C. **20**, 3621 (1987).
[14] R. A. Friesner and R. M. Levy, J. Chem. Phys. **80**, 4488 (1984).
[15] M. F. Herman, E. J. Bruskin, and B. J. Berne, J. Chem. Phys. **76**, 5150 (1982).